NUMERICAL SIMULATIONS OF SUPPRESSION EFFECT OF WATER MIST ON HYDROGEN DEFLAGRATION IN CONFINED SPACES

Xu, Zhanjie [1], Zhang, Zhi [2], Kotchourko, Alexei [3] and Lelyakin, Alexander [4]
Karlsruhe Institute of Technology, P.O. Box 3640, 76021 Karlsruhe, Germany
[1]zhanjie.xu@kit.edu, [2]zhangzhi@mail.hfut.edu.cn, [3]alexei.kotchourko@kit.edu,
[4]alexander.lelyakin@kit.edu

ABSTRACT

Hydrogen safety issues attract focuses increasingly as more and more hydrogen powered vehicles are going to be operated in traffic infrastructures of different kinds like tunnels. Due to the confinement feature of traffic tunnels, hydrogen deflagration may pose a risk when a hydrogen leak event occurs in a tunnel, e.g., failure of the hydrogen storage system caused by a car accident in a tunnel. A water injection system can be designed in tunnels as a mitigation measure to suppress the pressure and thermal loads of hydrogen combustion in accident scenarios. The COM3D is a fully verified three-dimensional finite-difference turbulent flow combustion code, which models gas mixing, hydrogen combustion and detonation in nuclear containment with mitigation device, or other confined facilities like vacuum vessel of fusion and semi-confined hydrogen facilities in industry, such as traffic tunnels, hydrogen refueling station etc. Therefore, by supporting of the European HyTunnel-CS project, the COM3D is applied to simulate numerically the hydrogen deflagration accident in a tunnel model, being suppressed by water mist injection. The suppression effect of water mist and the suppression mechanism is elaborated and discussed in the study.

Key Words: confined space; tunnel; hydrogen deflagration; hydrogen safety; water injection; water mist; hydrogen- powered vehicle.

1 INTRODUCTION

Tunnels are an increasingly important part of the traffic infrastructure especially in territorially uneven mountain areas. They create challenges for prevention and management of incidents/ accidents, fire and explosion protection and security against attacks or sabotage. The use of alternative fuels, including compressed gaseous hydrogen (CGH2) and cryogenic liquid hydrogen (LH2), in tunnels and similar confined spaces creates new challenges to provision of life safety, property and environment protection at acceptable level of risk.

The confined feature of traffic tunnel may amplify the potential risk of hydrogen fuel cell vehicles (HFCVs) in accident scenarios. Due to the narrow space and auxiliary facilities and devices acting as blockages in tunnel, the tube might become an ideal place for hydrogen flame acceleration even detonation if the hydrogen involved accidents are not properly mitigated. Ventilations are designed for tunnels traditionally, to purify contaminants in air in normal operation and to control smoke in hydrogen-carbon fires caused by, e.g., conventional petroleum product fuelled vehicle accidents. In case of HFCV accident, ventilation can also facilitate to disperse and exhaust unintentionally released hydrogen.

Another important mitigation measure is water spray or mist in tunnels, which can decrease fire growth, spread and heat release rate of tunnel fires due to its cooling effect. It is an interesting topic to study the interaction between the distributed liquid droplets and hydrogen behaviours in tunnels.

Numerical modelling and CFD simulations of hydrogen distribution and combustion in tunnels or tunnel-like facilities were performed without water intervention e.g., in the literatures [1– 5]. This study focuses on hydrogen deflagration suppressed by water mist in a tunnel.

2 GEOMETRICAL MODELS

The experimental tunnel is modelled, which is a 70 m long and 3.7 m diameter explosion testing facility located at the Health and Safety Executive's (HSE) laboratory in the UK. The whole view of the tunnel model is shown in Fig. 1, which nominal dimension is 70 m long, 3.7 m wide and 3.4 m high. The circular profile of the cross section of the tunnel structure has a diameter of 3.8 m in model.

In total, nine properly scaled vehicles are modelled, including seven cars, a van and a bus. They are arranged in two columns in the tunnel. Four cars are in one lane; the other three together with the van and the bus are in another lane. Each vehicle is located at the centre of each lane with a uniform spacing distance of about 1 m, except the first car. It is assumed as the failed HFCV, thus, has a larger distance to the second car behind. The dimensions of the car, the van and the bus models are $2\times0.9\times0.6$ m^3, $2.4\times0.9\times1.1$ m^3 and $4.5\times1.1\times1.6$ m^3, respectively. For laboratory convenience, each column of vehicles are placed on two parallel rails, which are 0.1 m high and separated by 0.5 m. The hydrogen injection location is beneath the chassis of the first car. The hydrogen release location is 35 m from the tunnel portal, namely, in the middle length of the facility.

The calculation domain is discretized into 880,600 numerical cells with a uniform cell size of 0.1 m.

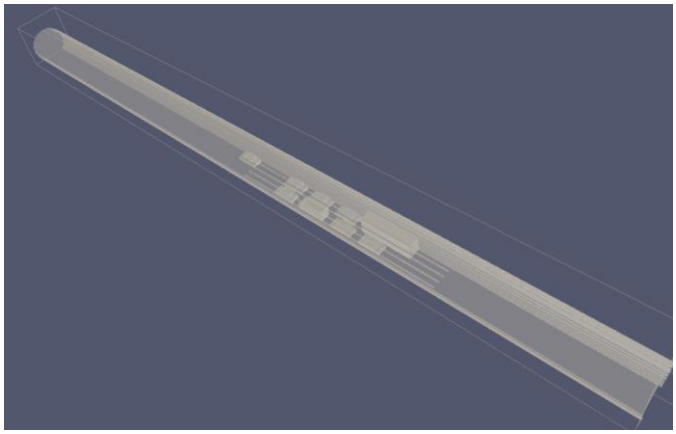

Figure 1. Geometrical model of tunnel facility with nine vehicles including cars, a van and a bus.

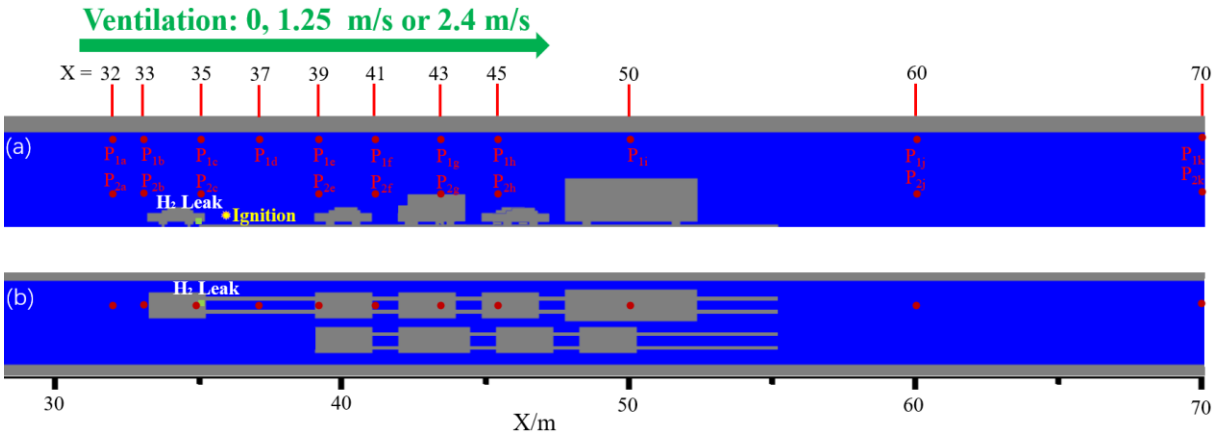

Figure 2. Computational domain views in a vertical cut (a) and in a horizontal cut (b), showing the layout of vehicle models and the positions of pressure gauges modelled in simulations.

The layout of the vehicle models are further presented in Fig. 2. To monitor pressure evolutions of hydrogen deflagration, two columns of pressure gauges are configured in simulations. The locations of the gauges in each column share the same height. The lower column is 1 m above the tunnel ground; the higher one is 3 m above the ground. Clearly all the gauges are located above the hydrogen leaking point.

The longitudinal x-coordinates of the pressure gauges are 32 m, 33 m, 35 m, 37 m, 39 m, 41 m, 43 m, 45 m, 50 m, 60 m, 70 m, respectively. The hydrogen leaking nozzle is beneath the first vehicle model counted from the left hand side, denoted as the small square in green in Fig. 2. The ignition point is defined at downstream at 0.8 m from the leak and at 0.5 m above the tunnel ground, denoted as the dot in yellow in Fig. 2 (a).

The tunnel can be vented in need by a longitudinal air flow from the left portal to the right. The ventilation flow velocity can be configured as 1.25 m/s or 2.4 m/s for the consideration of variant venting efficiencies.

3 MODEL DESCRIPTIONS

3.1 COM3D code

The COMD3D code is a finite difference code dedicated to simulate gas mixing and turbulent combustion including explosion and detonation in complex large-scale industrial facilities. Based on well established numerical practice the compressible Navier-Stokes equations are solved in three-dimensional Cartesian space to reproduce flow filed details. By solving the governing equations of momentum, total energy and mass, and transport equations of each species, the code offers 3D fluid dynamic distributions of species, velocity, density, turbulence and discrete particles, and thermodynamic parameters of pressure and temperature [6].

3.2 Simplified two-phase flow

Hydrogen deflagration and detonation is a fast process, always takes place in a relatively short time e.g., less than 0.5 s in the studied case of deflagration in the tunnel model. According to the estimations of heat absorption by droplets [7], thermal process and phase change are relatively slow comparing to fast combustion processes including deflagration and detonation. Therefore, vaporization or condensation is ignored in the study. It is assumed that the liquid droplets distribute uniformly in a computing cell. The liquid phase is treated like a normal gas species while solving the total energy equation. The treatment can be called as a simplified homogeneous two-phase flow model.

3.3 Lagrangian particle model

According to the Lagrangian particle model assumptions, the liquid droplets are modelled as discrete entities, which can be entrained and transported by the accompanying gas flow. The aerodynamic drag force is the main contributor to entrain a particle. The particle momentum equation is shown as follows.

$$\frac{dm_d\overrightarrow{v_d}}{dt} = m_d\vec{g} - \frac{1}{2}\rho_g C_D \pi {r_d}^2 \|\overrightarrow{v_{rel}}\|\overrightarrow{v_{rel}} \quad (1)$$

where,

m_d: droplet or particle mass, kg,
$\overrightarrow{v_d}$: droplet velocity, m/s,
r_d: droplet radius, m,
ρ_g: surrounding gas density, kg/m^3,
C_D: drag coefficient, which is a function of Reynolds number of droplet,
$\overrightarrow{v_{rel}}$: droplet velocity relative to gas, m/s.

The liquid phase is transported in form of droplets (particles) by solving the particle dynamic equations.

4 SIMULATIONS

4.1 Hydrogen source and ignition

It is assumed that hydrogen is released adiabatically from a scaled high pressure storage tank, with a volume of 0.053 m^3 at a pressure of 118 bar. Notional nozzle concept is applied to determine the hydrogen blowdown dynamics. The mass flow rate and the temperature of hydrogen source at the effective nozzle are shown in Fig. 3, as a boundary condition for simulations. Such an assumption is equivalent to a TPRD nozzle diameter of 2.24 mm for hydrogen release. The direction of hydrogen injection is assumed downwards to the ground.

As mentioned in Section 2, a numerical mesh of 0.1 m cell size is configured to model the 70 m long tunnel, due to limited computing resource. Such a coarse mesh cannot reproduce the detailed feature of a blowdown jet flow, e.g., with a partial loss of the jet momentum. However, the simplification does not influence the main task to study the deflagration of the dispersed hydrogen cloud, which is the main goal of the study.

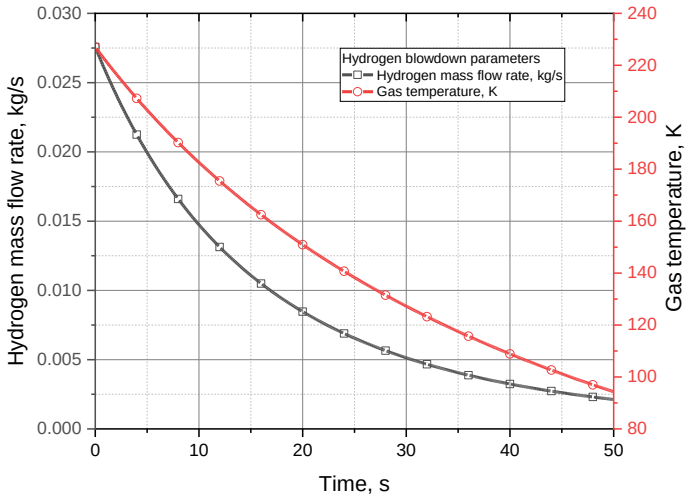

Figure 3. Adiabatic H_2 blowdown parameters at effective nozzle: mass flow rate (kg/s) and temperature (K), approximately equivalent to H_2 release through a TPRD nozzle diameter of 2.24 mm from a storage tank of 0.053 m^3 at 118 bar.

The timing to ignite the dynamically developing hydrogen cloud is selected by considerations. It is defined with attempts to find the worst case as possible, when the ignited cloud may generate the highest overpressure of hydrogen deflagration. Due to the decaying character of the blowdown mass flux and the enhanced hydrogen dispersion by ventilation, it was found after many tryouts that the highest overpressure of combustion occurs neither in the case of too late ignitions nor the case of too early ignitions. Thus, the timings for ignition are determined at 2.5 s, 5.1 s or 9.2 s, with 0 s defined at the starting moment of hydrogen blowdown.

4.2 Water mist configuration

Water mist is configured to fill the whole gas volume of the tunnel section between the left end of the first vehicle to the right end of the last bus model, as shown in Fig. 4. The configuration is certainly an idealized scenario mimicking a pre-misted region in the test facility. In a real tunnel operation, the misted region can be formed only after mist generators are activated by a detection signal of hydrogen release. A droplet diameter of 500 µm and a liquid phase (water) concentration of 10 kg/m^3 are defined, which lead to 2.9×10^{10} *real* droplets in total. It is clearly not feasible to simulate every single droplet of such

a huge number. Therefore, a model of droplet multiplication factor has been developed for the code. The factor determines the number of *real* droplets that are initialized in one cell and are calculated collectively. By specifying a droplet multiplication factor of 1.45×10^6, only a number of 20,000 *simulating* droplets are calculated representatively. The droplets are still initially at a temperature of 298 K.

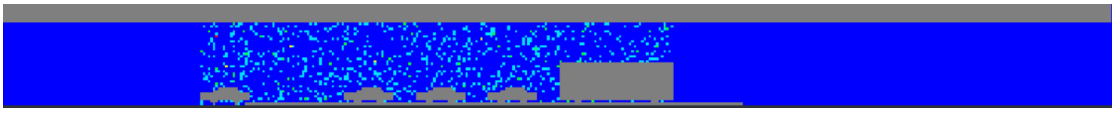

Figure 4. Misted region in the tunnel.

4.3 Boundary and initial conditions

Common boundary conditions for simulations are: ambient temperature: 298 K; ambient pressure: 1.013×10^5 Pa; gravity: 9.81 m/s^2; ventilation velocity (horizontally from left to right): 0 m/s, 1.25 m/s or 2.4 m/s.

By considering the variables, a simulation case matrix is summarized in Table 1.

Table 1 Simulation cases with variant ventilations and ignition times with or without water mist

	Without mist			With mist
Ignition time / Ventilation	2.5 s	5.1 s	9.2 s	5.1 s
0 m/s	A	B	C	J
1.25 m/s	D	E	F	K
2.4 m/s	G	H	I	L

The 12 scenarios listed in Table 1 are simulated by using the COM3D code. Hydrogen concentrations and overpressures caused by hydrogen deflagration are computed as results to analyze the mitigation effect of ventilation and water mist in different configurations.

4.4 Results

4.4.1 Ventilation influence on hydrogen distribution

As the starting case, hydrogen distribution is simulated without ventilation. The growing hydrogen cloud is shown in Fig. 5 at different evolution times. Due to the downward injection of hydrogen, the jet flow impinges on the tunnel ground and loses most momentum. The released hydrogen disperses beneath the vehicle chassis, as shown in Fig. 6. Then hydrogen arises around the vehicle due to the dominated buoyancy, until the cloud front touches the tunnel ceiling, where hydrogen continues to spread in both directions. Hydrogen is accumulated obviously on the ceiling and a layered and steady flammable mixture is formed there.

In case of the 1.25 m/s ventilation, the evolutional hydrogen concentration contour plots are shown in Fig. 7. It shows that almost all the released hydrogen is blown to the downstream of the ventilation flow. The hydrogen distribution in the horizontal cut below the chassis, as shown in Fig. 8, indicts the same tendency. Fig. 7 shows that, the hydrogen cloud arises because of its lighter density while it is entrained by the ventilation flow towards the downstream. Thus, the contacting point of hydrogen cloud on the

ceiling is shifted by about 2.5 m downstream due the ventilation. Fig. 7 (b, c, d) shows that, only a small fraction of hydrogen diffuses backwards to upstream while major cloud spreads along the ceiling to downstream. A continuous flammable hydrogen-air mixture is formed on the ceiling.

If the ventilation is enhanced to 2.4 m/s, the developing process of hydrogen cloud is shown in Fig. 9 and the hydrogen distribution in a horizontal cut below the chassis in Fig. 10. Due to the strong ventilation, the released hydrogen is dispersed effectively and the front profile of the hydrogen cloud is not stable. There is no serious accumulation of hydrogen on the ceiling. Fig. 10 indicates that the leaking hydrogen has no chance to distribute beneath the chassis, being vented away to the downstream instead and arising upwards.

By comparing Fig. 5 and 7, it seems that the dimension of hydrogen cloud with a concentration e.g., >30 vol.% H_2 in Fig. 7 is larger than that in Fig. 5. It can be explained that the hydrogen disperses only in one direction (downstream) in the tunnel in case of ventilation, but the hydrogen disperses in both directions in case of no ventilation. In other words, the hydrogen concentration in the downstream region may be doubled somehow by the ventilation. It is quite certain that the dimension of hydrogen cloud with a concentration >30 vol.% H_2 in Fig. 9 is smaller than that of Fig. 7, because of the stronger mixing caused by the enhanced ventilation in the case of Fig. 9.

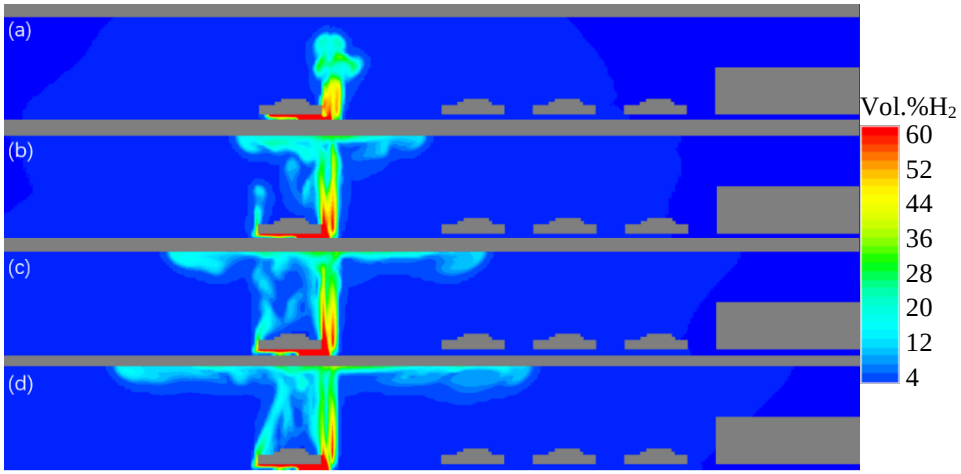

Figure 5. Hydrogen concentration contours in a longitudinal vertical cut through TPRD nozzle without ventilation at t = (a) 2.5 s; (b) 5 s; (c) 7 s; (d) 9 s.

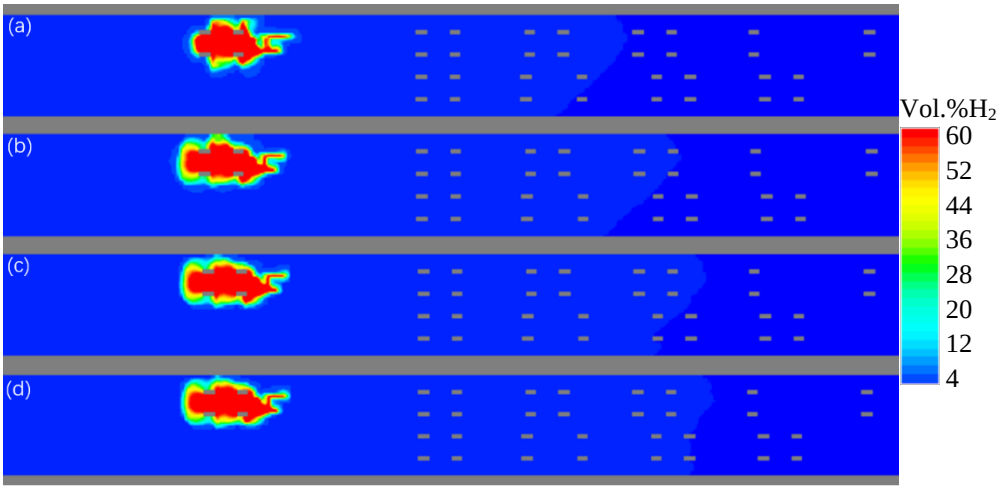

Figure 6. Hydrogen concentration contours in a horizontal view right below the chassis of the leaking vehicle without ventilation at t = (a) 2.5 s; (b) 5 s; (c) 7 s; (d) 9 s.

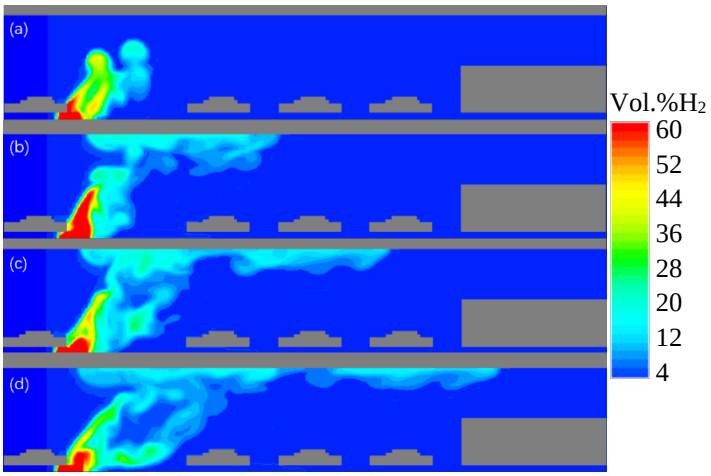

Figure 7. Hydrogen concentration contours in a longitudinal vertical cut through TPRD nozzle with 1.25 m/s ventilation at t = (a) 2.5 s; (b) 5 s; (c) 7 s; (d) 9 s.

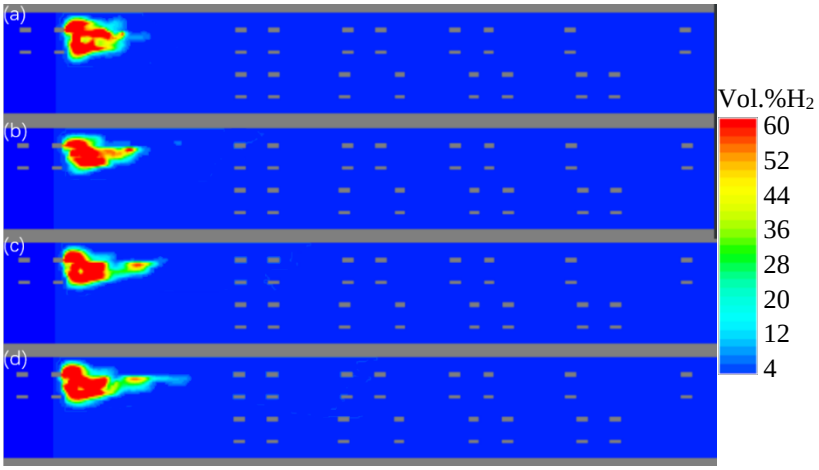

Figure 8. Hydrogen concentration contours in a horizontal view right below the chassis of the leaking vehicle with 1.25 m/s ventilation at t = (a) 2.5 s; (b) 5 s; (c) 7 s; (d) 9 s

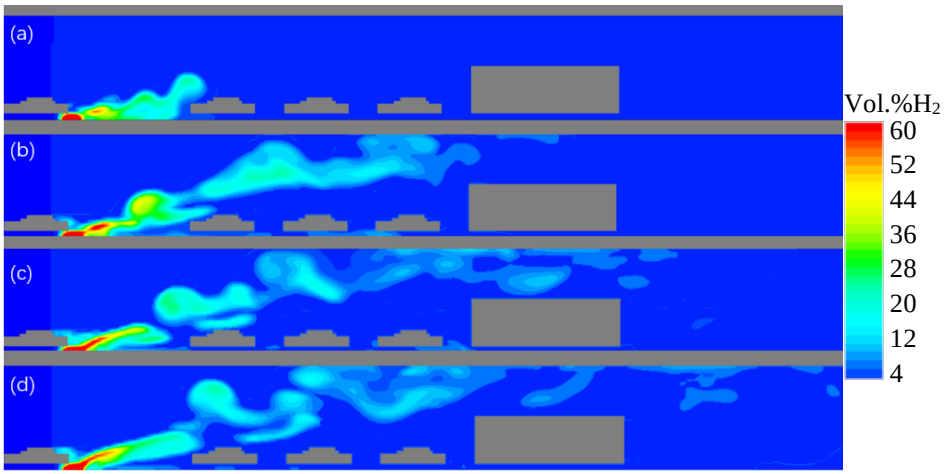

Figure 9. Hydrogen concentration contours in a longitudinal vertical cut through TPRD nozzle with 2.4 m/s ventilation at t = (a) 2.5 s; (b) 5 s; (c) 7 s; (d) 9 s.

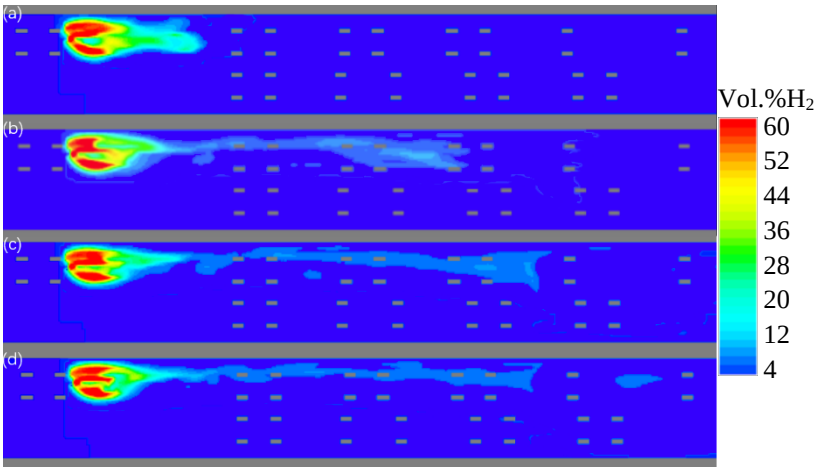

Figure 10. Hydrogen concentration contours in a horizontal view right below the chassis of the leaking vehicle with 2.4m/s ventilation at t = (a) 2.5 s; (b) 5 s; (c) 7 s; (d) 9 s.

4.4.2 Hydrogen deflagration without mist

The distributed hydrogen cloud in the tunnel is ignited without interfering of water mist. The overpressures caused by hydrogen combustion is computed with a ventilation velocity of 0 m/s, 1.25 m/s and 2.4 m/s, and an ignition time at 2.5 s, 5.1 s, and 9.2 s, respectively. The influence of ventilation on the hydrogen combustion overpressure is discussed in this subsection. Meanwhile, the results supply a base for comparison to the cases with water intervention addressed in next subsection.

Attention is focused on the overpressure produced by the hydrogen combustions in different cases. The two columns of pressure gauges are defined in the model, as shown in Fig. 2. They record the local pressure time histories in the combustion field. The peak overpressure is obtained among the recordings of the gauges.

The nine combinations of three ventilation efficiencies by three ignition times define nine simulation cases without mist. The hydrogen combustion overpressures in the nine cases are listed in Table 2. According to the table, the highest overpressure occurs in the cases with the ignition time of 5.2 s if ventilation is available. Therefore, the pressure evolutions are address in details for the three cases with the ignition time of 5.2 s.

The overpressure histories are shown in Fig. 11 – 13, for the ventilation air flow velocity of 0 m/s, 1.25 m/s and 2.4 m/s, respectively. The plots show the peak overpressures of combustion and the pressure front propagations along the tunnel. For an instance, an overpressure of 2000 Pa is indicated in Fig. 11, which is recorded by the gauge P_{1a} located at X = 37 m and 3 m above the ground. A fast combustion can produce pressure shock even the flame speed is subsonic. The traveling process of pressure front is clearly reproduced in Fig. 11. E.g., the peak pressure arrives at the gauge P_{1d} (X=37 m) at 5.1155 s, P_{1i} (X=50 m) at 5.1505 s, and P_{1k} (X=70 m) at 5.2071 s. The propagating speed is about 371 m/s from the gauge P_{1d} to P_{1i}, and 353 m/s from P_{1i} to P_{1k}, averagely 360 m/s from P_{1d} to P_{1k}. The speed manifests that only deflagration occurs in the tunnel without detonation, which features normally in a supersonic speed. Actually, the subsonic flame front decelerates a little, namely, from 371 to 353 m/s, because the hydrogen fraction decays along the distance from the leaking location. The maximum overpressure is recorded as 2075 Pa for the case without ventilation, by the gauge P_{2b}, as shown by the curve in red in the second plot of Fig. 11.

In the case of 1.25 m/s ventilation, as shown in Fig. 12, the maximum overpressure is denoted by the gauge P_{1d} as 5305 Pa. It is interesting that, the peak overpressure is higher than that of the case without

ventilation. It is consistent with the judgement made in Section 4.4.1, that a higher concentration of hydrogen cloud is formed due to the longitudinal ventilation. Therefore, its combustion produces a higher overpressure. The drawback of singular longitudinal ventilation measure for traffic tunnels can be eliminated practically by using a hybrid ventilation system combining both longitudinal jet fans and transverse venting ducts. Fig. 12 also shows that the average flame speed is about 372 m/s from P_{1d} to P_{1k}. It is certainly subsonic in the deflagration regime.

When the ventilation velocity is increased to 2.4 m/s, the predicted peak overpressure is 4909 Pa, recorded by the gauge P_{1c} as shown in Fig. 13. The stronger mixing between hydrogen and air brings a lower H_2 concentration and a lower peak pressure. However, according to Fig. 13, the traveling speed of the pressure front is coincidently the same (about 372 m/s) as that in the case of 1.25 m/s ventilation. This may be explained by the compromise between the intensified turbulence and the lowered H_2 concentration. The both are the consequences of the stronger ventilation. However, the former promotes combustion and the latter suppresses. The result manifests the stochastic character of turbulent combustion process.

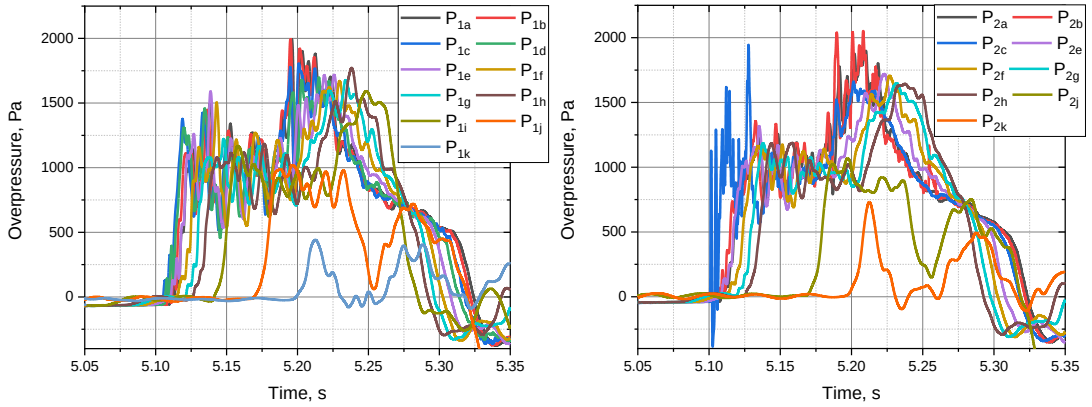

Figure 11. Overpressures in case of ignition time of 5.1 s without ventilation, without mist.

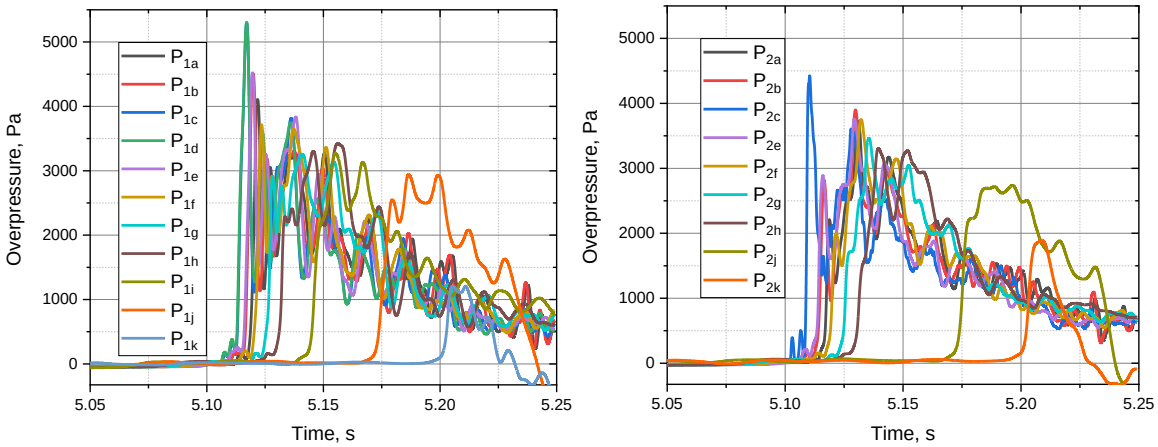

Figure 12. Overpressures in case of ignition time of 5.1 s with 1.25 m/s ventilation, without mist.

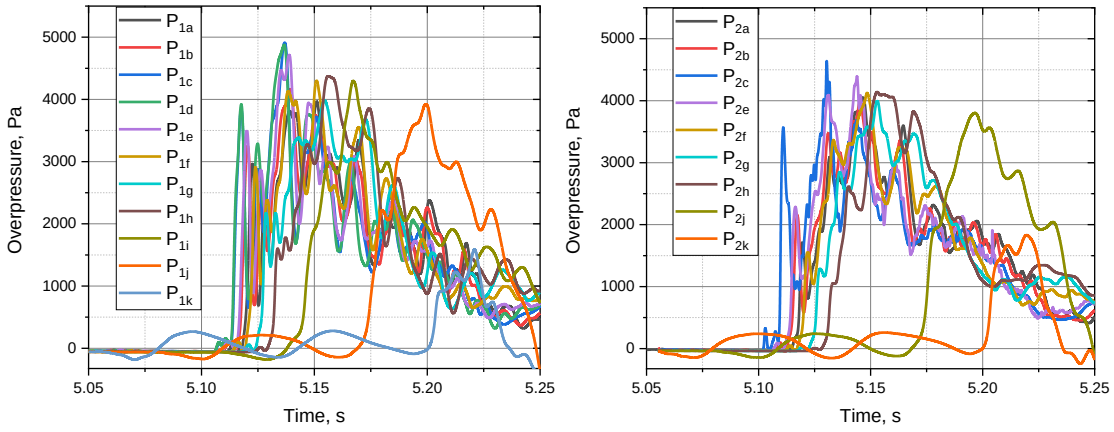

Figure 13. Overpressures in case of ignition time of 5.1 s with 2.4 m/s ventilation, without mist.

4.4.3 Mist influence on hydrogen deflagration

The mist is superimposed in the tunnel region with vehicle models at the igniting moment (5.2 s) for the three cases discussed in last section, respectively, to mimic the firefighting action in a tunnel fire accident. The interaction between hydrogen deflagration and water mist is simulated. The results about overpressures are shown in Fig. 14 – 16.

The maximum overpressures are summarized in Table 2 with the last column referring to the mist intervention cases. As shown in the figures and the table, the peak overpressures of combustion are 1413 Pa, 3058 Pa and 3294 Pa for the cases of 0 m/s, 1.25 m/s and 2.4 m/s ventilation, respectively. The overpressures are apparently lower than the corresponding values without mist, approximately by 32% – 42 %. The suppression effect of water mist on hydrogen combustion is quite obvious, primarily due to the following two factors: the cooling effect of water on the hot gases of combustion, and the hydrodynamic effect of the heavier density of the two-phase flow (H_2-air mixture plus liquid), which is about 9 times heavier than normal air by considering the imposed mist density of 10 kg/m^3.

The momentum suppression of the heavier two-phase fluid mixture is proved by the decreases of the propagation speeds of the pressure fronts in the three cases. According to the pressure records between the gauge P_{1d} and P_{1k} in Fig. 14 – 16, the combustion pressure wave travels at a speed of about 356 m/s, 365 m/s and 357 m/s, respectively, for the cases of 0 m/s, 1.25 m/s and 2.4 m/s ventilation. The all speeds are smaller, though slightly, than the corresponding values without mist analysed in last section.

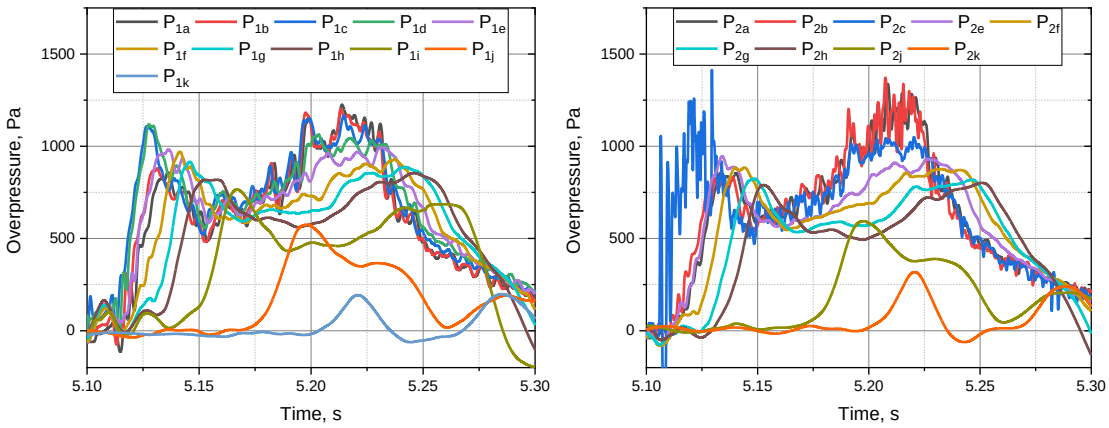

Figure 14. Overpressures in case of ignition time of 5.1 s without ventilation, with mist.

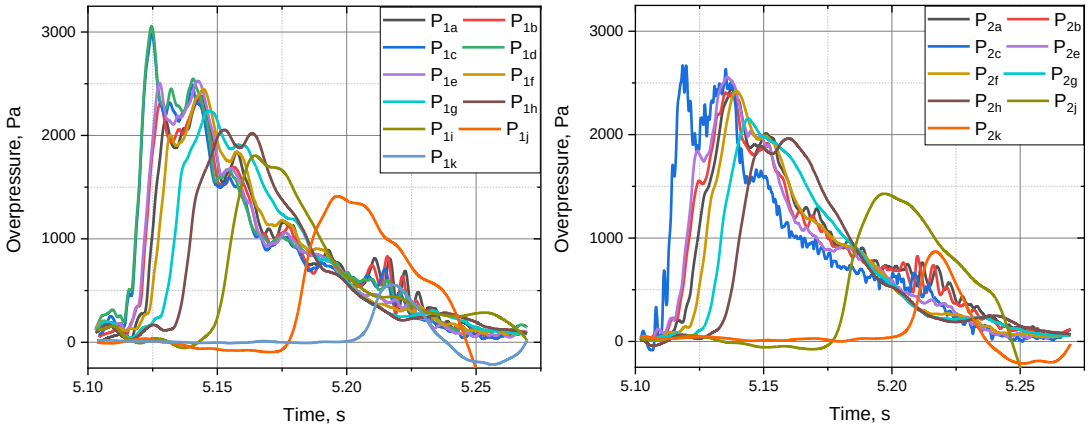

Figure 15. Overpressures in case of ignition time of 5.1 s with 1.25 m/s ventilation, with mist.

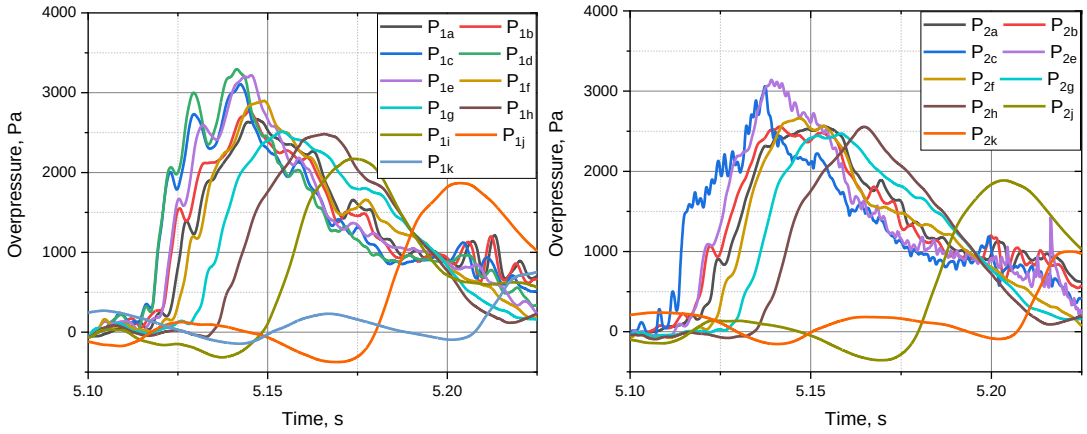

Figure 16. Overpressures in case of ignition time of 5.1 s with 2.4 m/s ventilation, with mist.

Table 2. Maximum overpressure for various cases

	Maximum overpressure: Pa			
	Without mist			With mist
Ignition time / Ventilation	2.5 s	5.1 s	9.2 s	5.1 s
0 m/s	2335	2075	1514	1413
1.25 m/s	4226	5305	3882	3058
2.4 m/s	4550	4909	4473	3294

Due to the relatively small release rate of hydrogen, the overpressures listed in Table 2 does not pose a serious threaten to human. However an overpressure of a few thousands pascal could bring a temporarily ear threshold shift.

5 CONCLUSION AND OUTLOOK

By applying a simplified water mist model into a computer code for turbulent combustion, the suppression effect of mist on hydrogen deflagration is studied for an experimental tunnel facility with different ventilation efficiencies and variant ignition times. The simulation results manifest that the overpressure of hydrogen combustion can be reduced by about 30-40 % if water mist is injected in a tunnel fire of hydrogen. The suppression effect is mainly contributed by the cooling effect of liquid water and by the hydrodynamic effect of the heavier density of the two-phase atmospheric flow.

Sensitivity studies on different injected water mist densities and droplet sizes are planned for next work. Hopefully, the relevant experiments would be performed to supply data to verify the numerical models.

ACKNOWLEDGMENT

The study is financially supported by the EU HyTunnel-CS project, which has received funding from the Fuel Cells and Hydrogen 2 Joint Undertaking (JU) under grant agreement No 826193. The JU receives support from the European Union's Horizon 2020 research and innovation programme and United Kingdom, Germany, Greece, Denmark, Spain, Italy, Netherlands, Belgium, France, Norway, Switzerland. The authors also appreciate the colleagues from the Health and Safety Executive's (HSE) laboratory in the UK, such as, M. Pursell, W. Rattigan etc. for geometrical information support about the explosion tunnel facility.

REFERENCES

1. I.C. Tolias, A.G. Venetsanos, N. Markatos, C.T. Kiranoudis, CFD modeling of hydrogen deflagration in a tunnel, International Journal of Hydrogen Energy, Volume 39, Issue 35, 3 December 2014, Pages 20538-20546.
2. D. Baraldi, A. Kotchourko, A. Lelyakin, J. Yanez, P. Middha, O.R. Hansen, A. Gavrikov, A. Efimenko, F. Verbecke, D. Makarov, V. Molkov, An inter-comparison exercise on CFD model capabilities to simulate hydrogen deflagrations in a tunnel, International Journal of Hydrogen Energy, Volume 34, Issue 18, September 2009, Pages 7862-7872.
3. Prankul Middh, Olav R. Hansen, CFD simulation study to investigate the risk from hydrogen vehicles in tunnels, International Journal of Hydrogen Energy, Volume 34, Issue 14, July 2009, Pages 5875-5886.
4. W. Breitung, U. Bielert, G. Necker, A. Veser, F.-J. Wetzel, K. Pehr, Numerical Simulation And Safety Evaluation Of Tunnel Accidents With A Hydrogen Powered Vehicle, 13th World Hydrogen Energy Conference, Beijing, China, June 12 – 15, 2000.
5. S. Kumar, S. Miles, P. Adams, M. Zenner, S. Ledin, A. Kotchourko, et al., HyTunnel: the use of hydrogen road vehicles in tunnels, Third International Conference on Hydrogen Safety, Ajaccio, Corsica, France, 16–18 September 2009.
6. A. Kotchourko, A. Lelyakin, J. Yanez, Z. Xu, K. Ren, COM3D: Turbulent Combustion Code Tutorial Guide Version 4.2, KIT, 2011.
7. J. Mohacsi, Study of attenuation effect of water droplets on shockwaves, Master Thesis, Karlsruhe Institute of Technology, Germany, Jan. 2020.